Interfacial electronic trap lifetimes studied by the photomodulation of second-harmonic generation processes

M. S. Yeganeh, J. Qi, and A. G. Yodh

Department of Physics, University of Pennsylvania, Philadelphia, Pennsylvania 19104

M. C. Tamargo*

Bellcore, 331 Newman Springs Road, Red Bank, New Jersey 07701

Received January 5, 1993; revised manuscript received May 21, 1993

Second-harmonic generation and linear photomodulation are combined to study free-charge trapping mechanisms at ZnSe–GaAs(001) heterointerfaces. The variation of second-harmonic intensity as a function of charged-trap density at the buried junction is analyzed quantitatively and used with time-dependent measurements to determine interfacial charge-trap lifetimes.

1. INTRODUCTION

Nearly 25 years ago Wang *et al.*[1] discovered that a secondary light beam can be used to improve dramatically the sensitivity of simple linear reflectance experiments. The photoreflectance method quickly became a routine spectroscopic diagnostic of semiconductors with space-charge regions.[2] Photoreflectivity offers high sensitivity to linear optical transitions with a narrow joint distribution of states. The secondary light beam generates electron–hole pairs (EHP's) whose injection into the material modulates the band bending and changes the joint density of states. Although the effect of optical carrier injection on linear spectroscopies is well understood, the analogous phenomenon in nonlinear optics has only recently attracted attention.[3,4] It is well known that second-order nonlinear optical probes are sensitive to the broken symmetries of a material system. This sensitivity has been used to study surfaces[5] and interfaces.[6–8] By analogy to linear reflectance, we might expect optical carrier generation in semiconductors to modulate the nonlinear response of the system. The nonlinear spectrum, for example, may be modified by carrier-induced changes of symmetry and energy eigenstates. Thus, we can in principle study interfaces with greater sensitivity.

In this paper we are interested in charge-trapping mechanisms at the interface between crystalline solids. It is well known that band bending at the junction of two dissimilar semiconductors can lead to new electronic states.[9,10] Recently we reported on the observation of such a state in ZnSe–GaAs(001) heterostructures when we used second-harmonic generation (SHG).[4] The second-harmonic spectral feature, at 2.72 eV, results from a virtual transition between the ZnSe valence band and a resonance state of a quantum well located across the junction in the GaAs conduction band. The interfacial quantum well, depicted in Fig. 1, develops as a result of band bending. The generation and trapping of carriers at this interface alters the junction band profile, the wave function of the interfacial quantum-well states, and the second-order nonlinear optical response of the system.

We have combined photomodulation with second-order nonlinear optics to study interfacial trap lifetimes at the ZnSe–GaAs(001) heterojunction. This contribution provides information about the effects of defects on free carriers and provides an example of how modulation techniques can be combined with nonlinear optical spectroscopies to provide low background information about interfaces. The quantities to which we are sensitive include the interfacial defect charge, density, location, and lifetime. Knowledge about these quantities is essential to fully understand charge transport and carrier lifetime in heterostructures, which in turn may help us to design better photodetectors, diode lasers, and light-emitting diodes.

The remainder of this paper is organized as follows. In Section 2 a theoretical background for the trapping mechanism and its effect on nonlinear optical signals will be given. The sample and experimental techniques will be described in Section 3. In Section 4 the results are presented, and a brief conclusion is given in Section 5.

2. THEORETICAL BACKGROUND

In our photomodulation second-harmonic generation (PSHG) measurements the sample was typically illuminated at normal incidence by light from a tungsten-lamp monochromator, while the SHG experiment was in progress (see Fig. 2). We have measured the intensity of the interfacial second-harmonic resonance at 2.72 eV as a function of lamp fluence and as a function of time after turning the lamp on and off. In this section we describe theoretical aspects of PSHG that pertain to the ZnSe–GaAs heterostructures. The mechanism underlying these experiments can be described as follows. The photogenerating light beam, with photon energy greater than the band gap of the system, produces EHP's.[11] Some of these free carriers move toward the junction and are captured by the interfacial trap centers, thereby altering the interface charge density. The new interface charge will modify the band bending and perturb the states associated with the quantum well. The interfacial trapped holes decrease the interface negative charge and decrease

0740-3224/93/112093-07$06.00

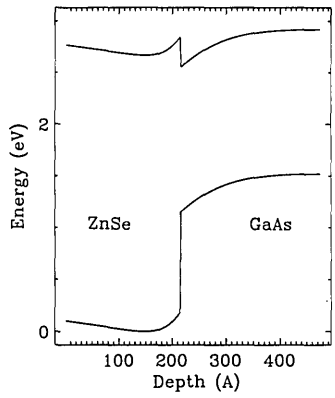

Fig. 1. Energy band profile as a function of depth for the ZnSe–GaAs(001) system. This band profile was determined by solving the Poisson equation for a Gaussian charge distribution. The thickness of the ZnSe overlayer is 21.5 nm.

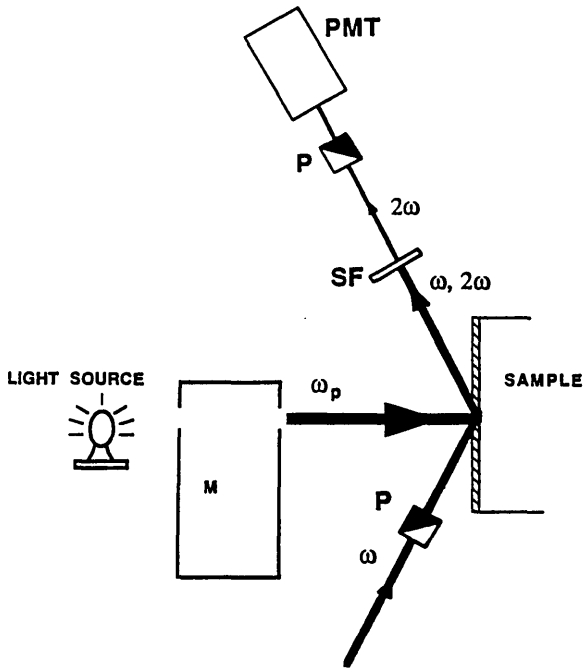

Fig. 2. Schematic of the PSHG experiment. The sample was illuminated at normal incidence by light from a tungsten-lamp monochromator while the SHG experiment was in progress: PMT, photomultiplier tube; P, polarizer; SF, spectral filter; M, monochromator; ω_p, angular frequency of photomodulating beam.

(increase) the band bending on the ZnSe (GaAs) side of the junction. This effect delocalizes the quantum-well wave function and reduces its relative amplitude within the well and depletion region. The amplitude of the valence band wave function, illustrated in the inset of Fig. 3(b), also reduces within the depletion region of the ZnSe overlayer. The reduction in amplitude produces a reduction in the oscillator strength for the transition between the valance band and quantum-well state. Alternatively, interfacial trapped electrons will increase the SHG signal. This theory is in agreement with our experimental observations and is consistent with our theoretical modeling,[12] the results of which are displayed in Fig. 3. In Fig. 3 we see that the change in the interfacial charge density primarily affects the wave function within the well and depletion region.

We have shown that the interfacial traps are predominantly hole traps.[4] This conclusion was deduced from measurements of second-harmonic intensity as a function of lamp photon energy, as displayed in Fig. 4. In this measurement the lamp intensity transmitted into the sample was held constant at 10 μW/cm^2. Although the efficiency of carrier generation in GaAs is much greater than that in ZnSe,[13] our data exhibited that the effect of photogenerated carriers in GaAs was negligible at this intensity. Because photoexcited electrons (holes) in GaAs (ZnSe) move toward the interface, we concluded that the interface traps are mainly hole traps. In this section we consider only the effect of hole traps; the arguments for electron traps are described in Appendix A.

Our goal is to calculate the photocarrier-induced change of the dominant second-order susceptibility tensor element, $\chi^{(2)}_{zzz}$.[14] This calculation will allow us to deduce the variation in second-harmonic intensity as a function of trapped-charge density and time. In the following discus-

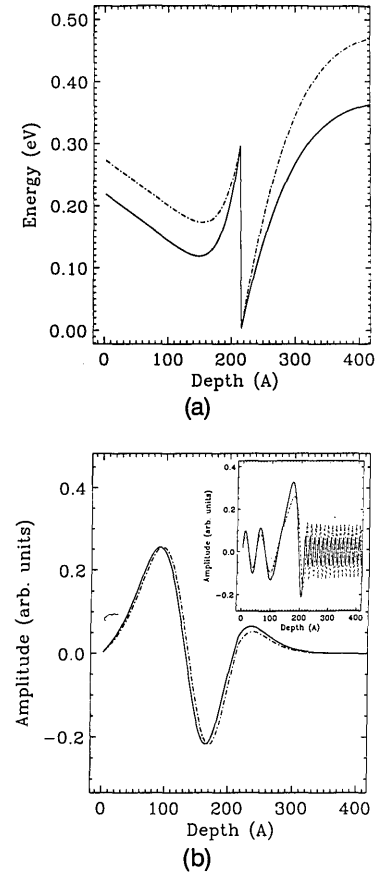

Fig. 3. (a) Variation of the conduction band profile with photomodulation. The variation was calculated on the basis of the creation of positive interface charge. The band bending increases (decreases) on the GaAs (ZnSe) side of the junction. The solid (broken) curve represents the band profile in the absence (presence) of the photomodulation light source. (b) Variation of quantum-well wave-function amplitude with photomodulation. The same variation for the valence band wave function is shown in the inset. The amplitude of the wave function within the well and the depletion region decreases. The solid (broken) curve represents the wave function in the absence (presence) of the photomodulation light source.

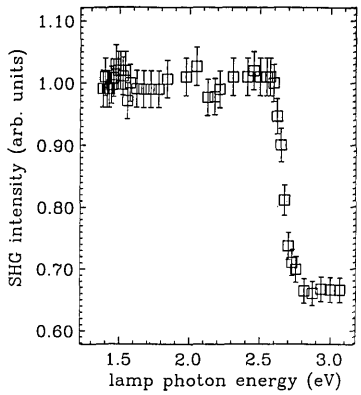

Fig. 4. Variation of the resonance interface SHG peak intensity at 2.72 eV as a function of lamp photon energy. The intensity transmitted into the sample was kept constant at 10 μW/cm^2.

sion we assume that the trap centers are localized at the junction, and we evaluate all the parameters at the interface. This assumption is reasonable because the interfacial imperfections are the main cause for the generation of trap centers. We also use the steady-state value of the free electron (n) and the free hole densities (p) for this calculation. Because our measured trap lifetime is many orders of magnitude greater that the lifetime of the free carriers, this assumption is also reasonable. Within this model the change in interface charge owing to trapping is proportional to the density of interfacial trapped holes, p_t. A rate equation at the interface relates p_t to the other physical parameters of the system[15,16]:

$$\frac{\partial p_t}{\partial t} = k_{1h}p(N_h - p_t) - k_{2h}np_t - r_h p_t. \tag{1}$$

Here N_h is the number density (number per square centimeter) of the interfacial hole trap centers and k_{1h} (k_{2h}) is the rate constant at which an unoccupied (occupied) trap center will trap a hole (recombine with an electron) at the interface. r_h is the rate constant at which a trapped hole is injected into the valence band by thermal excitation. In the low lamp excitation limit we assume that the densities of photogenerated carriers are linearly proportional to the intensity of the photogenerating lamp light, I_l. This linear approximation was experimentally tested and will be discussed later. Within the linear approximation we write

$$p = \alpha_{1h}I_l + p_0, \tag{2}$$

$$n = \alpha_{2h}I_l + n_0. \tag{3}$$

Here $\alpha_{1h}(\alpha_{2h})$ represents the deviation of interfacial free hole (electron) density from its thermal equilibrium value per unit lamp light intensity. Both α_{1h} and α_{2h} depend on the generation of free carriers and their transport to the interface. These parameters are a function of the quantum efficiency and mobility of the system. The equilibrium value of the free hole (electron) density in the absence of the photoexciting light is $p_0(n_0)$. Because thermal excitation probabilities in wide band-gap semiconductors are very small, we safely ignore the density of thermally excited holes, p_0, in comparison with photogenerated holes, $\alpha_{1h}I_l$, for photon energies greater than 2.67 eV.

The rate equation, Eq. (1), leads to the following time-dependent trapped-hole density:

$$p_t(t) = A_h \exp(-t/\tau_h) + \frac{k_{1h}\alpha_{1h}N_h\tau_{dh}I_l}{1 + I_l/I_{ch}}, \tag{4}$$

with

$$I_{ch} = \frac{1}{(k_{1h}\alpha_{1h} + k_{2h}\alpha_{2h})\tau_{dh}}, \tag{5}$$

$$\tau_{dh} = \frac{1}{k_{2h}n_0 + r_h}, \tag{6}$$

$$\tau_h = \frac{\tau_{dh}}{1 + I_l/I_{ch}}. \tag{7}$$

Here $\tau_h(\tau_{dh})$ is the interfacial charging (discharging) time. The parameter τ_{dh} is the trap lifetime at the junction. The charging intensity for hole traps, I_{ch}, is the photomodulating light intensity that produces a charging time of $\tau_{dh}/2$ in the system. Subscripts h indicate the value of a hole-trap parameter. A_h is a constant and is determined by initial conditions.

Two different initial conditions were used in our time-dependent measurements. These conditions lead to different values for the parameters in Eq. (4) and are described as follows. In the first case, the photomodulating light illuminating the sample is turned on at $t = 0$, and the initial density of trapped holes is zero. Under these conditions the value of A_h is

$$A_h = -\frac{k_{1h}\alpha_{1h}N_h\tau_{dh}I_l}{1 + I_l/I_{ch}}. \tag{8}$$

In the second case, the sample was illuminated for a long time and then the photomodulating lamp source was turned off at $t = 0$. In this case A_h represents the value of hole trapped density at $t = 0$, and the intensity of light source is zero. Thus, Eq. (4) reduces to

$$p_t(t) = p_{t_0} \exp(-t/\tau_{dh}). \tag{9}$$

The time-dependent Hamiltonian resulting from this interfacial trapped charge is approximately

$$H_h^{(1)} = \frac{2\pi e}{\epsilon} q_h p_t(z - d), \tag{10}$$

where $\hat{z}$ is in the direction normal to the interface, $q_h(e)$ is the unit charge of a hole (electron), and d is the thickness of the ZnSe overlayer. The effect of this Hamiltonian on the electronic structure of the system and $\chi^{(2)}_{zzz}$ can be described by perturbation theory. Because the measured time scale for the change in $\chi^{(2)}_{zzz}$ was much slower than the electronic lifetime of the quantum-well states, we can use time-independent perturbation theory to explain the physical phenomena in our calculations.

The wave function of the interfacial quantum well is sensitive to the detailed structure of the well and thus to the band bending at the junction. We expect states that are most sensitive to the photomodulation effects to be those whose existence depends strongly on the interfacial quantum well. For example no change in the bulk SHG signal was observed under photomodulation.[8] The varia-

tion of $\chi^{(2)}_{zzz}$ may thus be reasonably modeled by considering only changes of the resonance state of the interfacial quantum-well wave function, $|w\rangle$.

Because the electrons in the conduction band are free in the plane parallel to the interface, the essential part of the Schrödinger equation for this system reduces to a one-dimensional problem. The eigenstates of this problem decay rapidly into the vacuum (that is, $z \to \infty$) and are nondegenerate.[17] Using nondegenerate perturbation theory, we have

$$|w\rangle = |w_0\rangle + \sum_{w'} \frac{\langle w'|H_h^{(1)}|w_0\rangle}{E_{w'w_0}}|w'\rangle. \tag{11}$$

The $|w'\rangle$ are other eigenstates of the quantum well,[12] and $|w_0\rangle$ represents the unperturbed state. The denominator $E_{w'w_0}$ denotes the difference between the energy eigenvalue of the state $|w'\rangle$ and the state $|w_0\rangle$. The average energy interval between these eigenvalues is ~28 meV,[12] and the states are taken as sharp lines in the energy spectrum. The perturbation leads to a first-order variation of the second-order susceptibility $\chi^{(2)}_{zzz}$,

$$\begin{aligned}\frac{\chi_{zzz}}{\chi_{zzz,0}} &= 1 + \sum_{w'} \frac{2\pi e q_h p_t}{\epsilon E_{w_o w'}} \\ &\times \left(\frac{\langle v|z|w'\rangle\langle w'|z|w_0\rangle}{\langle v|z|w_0\rangle} + \frac{\langle w_0|z|w'\rangle\langle w'|z|e\rangle}{\langle w_0|z|e\rangle} \right) \\ &\equiv 1 + M_h p_t,\end{aligned} \tag{12}$$

with

$$M_h \equiv \sum_{w'} \frac{2\pi e q_h}{\epsilon E_{w_o w'}} \left(\frac{\langle v|z|w'\rangle\langle w'|z|w_0\rangle}{\langle v|z|w_0\rangle} + \frac{\langle w_0|z|w'\rangle\langle w'|z|e\rangle}{\langle w_0|z|e\rangle} \right). \tag{13}$$

The states $|v\rangle$ and $|e\rangle$ represent the valence band and a higher energy (that is, above the ZnSe conduction band) excited state, respectively. Equation (11) and identity (12) determine the fractional SHG intensity variation, that is,

$$\frac{I^{(2\omega)}}{I_0^{(2\omega)}} = [1 + C_{1h} + C_{2h} \exp(-t/\tau_h)]^2. \tag{14}$$

Here

$$C_{1h} = \frac{M_h k_{1h} \alpha_{1h} N_h \tau_{dh} I_l}{1 + I_l/I_{ch}}, \tag{15}$$

$$C_{2h} = M_h A_h, \tag{16}$$

where $I^{(2\omega)}$ [$I_0^{(2\omega)}$] is the second-harmonic intensity in the presence (absence) of a photoexciting light source. The wave function for the one-dimensional problem under investigation is chosen to be real[17]; therefore, C_{1h} and C_{2h} are also real. C_{1h}/M_h is the steady-state solution for the trapped-hole density [Eq. (1)]. Equation (14) shows that the trapped-charge density increases with the lamp intensity and approaches its asymptotic value, $k_{1h}\alpha_{1h}N_h\tau_{dh}I_{ch}$. At this point the charge density, p_t, will not be affected by higher lamp intensity and the band flattening will have reached its final condition. This steady-state solution of the trapped-hole density was recently used to deduce the relative trap density in ZnSe–GaAs samples.[4]

Within our experimental resolution of 6 meV at 915 nm, we did not observe any energy shift in the second-harmonic spectra under the photomodulation. This observation results from the fact that both the resonance state of the quantum well and the ZnSe band profile shift upward in energy as a result of the photomodulation. The upward shifts are almost the same, so that only a very small variation (~1 meV) in the transition energy of the SHG resonance arises. Our computations[12] predict spectral shifts of less than ~2 meV.

3. EXPERIMENTS

Our ZnSe–GaAs(001) heterostructure sample consists of a 21.5-nm epitaxial layer of undoped ZnSe(001) grown on a 0.5-μm undoped GaAs(001) film terminated with 2×4 surface reconstruction. The details of the growth and characterization are described in Ref. 18. A schematic of the PSHG experiment is shown in Fig. 2. A tungsten-lamp monochromator was the photomodulating light source. It was replaced by an Ar^+ laser whenever an intense beam was required. Details of the SHG experiments on ZnSe–GaAs(001) are given in Ref. 19. Note that a Nd:YAG-pumped dye laser with a repetition rate of 10 Hz was the light source for second-harmonic measurements, and the boxcar averager was set to take an average over 10 shots. This method brings the time resolution of the experiments to ~1 s.

The time-dependent PSHG experiments were designed to measure the trap lifetimes, τ_{dh} and τ_{de}, and charging time, τ_h. The steady-state PSHG experiments were used to study the dependence of the charging time on photomodulating light intensity. The time-dependent measurements were performed by the use of two different initial conditions: an open and a closed photogenerating beam shutter. To measure the intensity dependence of charging time, τ_h, we illuminated the sample with light at a fixed intensity, and the second-harmonic signal was measured as a function of time. This procedure was carried out for different lamp intensities and was repeated 100 times at each fluence.

The measurements of trap lifetime were carried out by the illumination of the sample with the lamp for at least 2 min. Then, the photogenerating beam shutter was closed, and the SHG intensity was measured as a function of time. This procedure was also repeated 100 times.

We also measured the steady-state second-harmonic intensity as a function of lamp fluence for a photon energy of 2.4 and 3.0 eV. In these measurements the sample was illuminated for a period of ~2 min to ensure that steady-state conditions were reached.

4. RESULTS

The experimental results of the hole and the electron trap lifetime (that is, τ_{dh} and τ_{de}) measurements are displayed in Fig. 5. The photon energy of the photomodulating beam used in the hole (electron) trap lifetime measurements was 3.0 eV (2.4 eV). The data exhibit a slow recovery time for the second-harmonic intensity in both cases. The solid curves in Fig. 5 are the best fit to the theory. Our fitting routine determined the best value for the recombination of the interfacial trap lifetime. This value was 35.4 ± 0.5 s and 35.0 ± 0.5 s for hole and electron trap

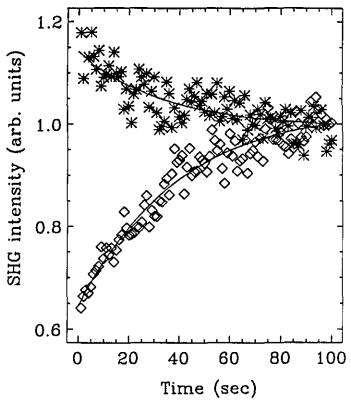

Fig. 5. Normalized second-harmonic intensity at lamp photon energies of 2.4 eV (*) and 3.0 eV (◇) as a function of time. The sample was illuminated by the photoexcitation beam for at least 2 min, then the photoexcitation shutter was closed (at $t = 0$) and data acquisition began.

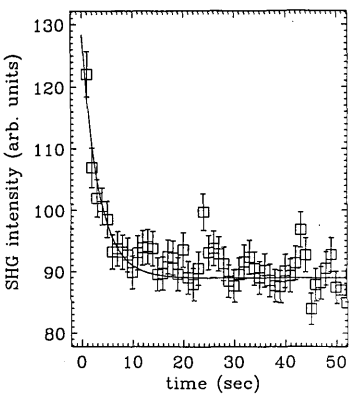

Fig. 6. Normalized second-harmonic intensity as a function of time. A photoexcitation beam with intensity 5.3 μW/cm^2 illuminated the sample at $t = 0$.

lifetime, respectively. These long lifetimes are characteristic of metastable electronic states typically generated by defects. Our results indicate that the lifetime for electrons and holes are the same within the experimental resolution. The surprisingly close values of the electron and the hole trap lifetimes are not intrinsic to our model, and we do not yet understand this result.

The variation of the resonance second-harmonic intensity as a function of time after the lamp is turned on is shown in Fig. 6. To investigate the intensity dependence of the interfacial charging time, we repeated this measurement for lamp intensities ranging from 0.4 μW/cm^2 to 5.3 μW/cm^2. We were not able to perform the time-dependent measurements at higher lamp intensities because higher intensities resulted in charging times that were shorter than the resolution of our apparatus.

The solid curve in Fig. 6 is the theoretical fit to the experimental data when we use Eq. (14). As expected the charging time decreased with increasing lamp illumination intensity. The optimum value for the free parameters C_{1h}, C_{2h} [Eqs. (15) and (16)] and charging time τ_h [Eq. (7)] were determined from our fits. The fitting was performed for all measured lamp intensities. In this way we were able to study the variation of the charging time as a function of lamp intensity. Our data, with lamp fluences below 5.3 μW/cm^2, demonstrated that the inverse of the charging time, and thus the free carrier densities, depended linearly on the intensity of the photoexciting beam. This linear relationship is displayed in Fig. 7. We also see that the inverse of τ_h approaches the trap lifetime (discharging time) as the lamp intensity approaches zero. These results justify the linear approximation used in our computation and lend support for our theoretical model. Using the τ_{dh} value we are able to deduce the value of 0.8 μW/cm^2 for I_{ch} [see Eq. (5)]. This intensity is also shown in Fig. 7. Our data demonstrate that the linear approximation holds for intensities up to $\sim 7 \times I_{ch}$ (5.3 μW/cm^2). This intensity is high enough to reduce the charging time by a factor of ~10 to our resolution limit but is still too weak to break the linear approximation.

We now turn to the dependence of the steady-state second-harmonic intensity on the photoexcitation fluence. The steady-state SHG intensity as a function of lamp intensity for a lamp photon energy of 3.0 eV is shown in Fig. 8. A word of caution is necessary in analyzing the data. Our theoretical results in Eq. (15) are based on a linear approximation, and our lifetime measurements are able to show linearity only up to 5.3 μW/cm^2. Thus, in principle, we can only fit our data for intensities below 5.3 μW/cm^2. The solid curve in Fig. 8 is the best fit when only the low intensity data are used. The constants $k_{1h}\alpha_{1h}N_h$ and I_{ch} are the only two free parameters in our fitting routine, and the value of $\tau_0^{-1} = kn_0 + r$ was deduced from the time-dependent measurements.

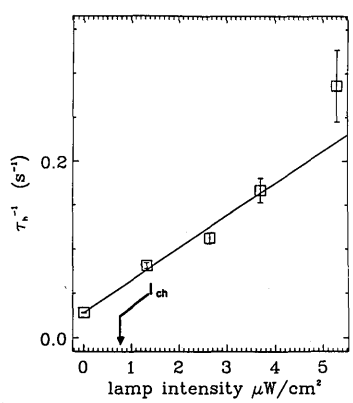

Fig. 7. The inverse of charging time (τ_h) as a function of the intensity. The solid line is the best fit to the data.

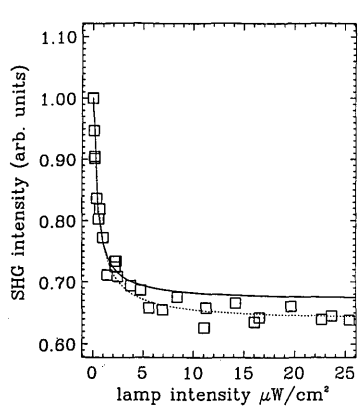

Fig. 8. The steady-state normalized second-harmonic intensity as a function of lamp intensity. The dotted curve is the best fit when all the available data are used, and the solid curve is the best fit when only the low intensity portion of the data is used.

We have carried out the fitting routine for all available data, shown by a dotted curve in Fig. 8. The comparison of these two fits illustrates the validity of the linear approximation at higher intensities. We can see that these two fits are different for high lamp intensities.

5. CONCLUSION

Linear photomodulation and SHG were combined as a new method to investigate solid–solid interfaces. Using this technique, we have studied trapping mechanisms at ZnSe–GaAs(001) heterointerfaces. This mechanism was formulated and used with the time-dependent measurements to deduce the lifetime of interfacial traps. The recombinations of the interfacial trap lifetime for holes and electrons were 35.4 ± 0.5 s and 35.0 ± 0.5 s, respectively. We have also demonstrated that the interfacial charging time depends on the intensity of the photomodulating light source. The inverse of the charging time was found to be a linear function of the light intensity for low lamp light intensity. Our steady-state PSHG data suggested that the linear approximation may not be suitable for intensities higher than ~8 μW/cm^2.

We believe that PSHG is a promising tool for the study of solid interfaces in the presence of band bending. We are currently exploring this technique for surface band bending of the semiconductors and on Schottky barrier heights in metal semiconductors. We are also investigating the effect of photomodulation on other nonlinear processes, such as Raman scattering. The results of these experiments will be described in future publications.

APPENDIX A: ELECTRON TRAPPING

Photogeneration of EHP with lamp photon energies less than the ZnSe band gap and greater than GaAs band gap will occur predominantly on the GaAs side of the heterostructure. Under these conditions electrons migrate toward the interface. Some of these carriers are captured by interfacial electron traps. In this appendix we are interested in calculating the deviation of the trapped electron density, δn_t, from its equilibrium value, n_{to}. The localized rate equation for n_t is

$$\frac{\partial n_t}{\partial t} = k_{1e} n (N_e - n_t) - k_{2e} p n_t - r_e n_t. \tag{A1}$$

The subscript e stands for electron, and the definition of each parameter is given for hole trap in the text. Equation (A1) leads to the time-dependent value of n_t. After subtracting the steady-state value of the trap density in the absence of light, n_{to}, we can write

$$\delta n_t = A_e \exp(-t/\tau_e) + \frac{k_{1e}(k_{2e} p_0 + r_e)\alpha_{2e} N_e \tau_{de}{}^2 I_l}{1 + I_l/I_{ce}}, \tag{A2}$$

where

$$\tau_e = \frac{\tau_{de}}{1 + I_l/I_{ce}}, \tag{A3}$$

with

$$I_{ce} = \frac{1}{\alpha_{2e} k_{1e} \tau_{de}}, \tag{A4}$$

$$\tau_{de} = \frac{1}{(k_{1e} n_0 + k_{2e} p_0 + r_e)}. \tag{A5}$$

The expression for the perturbation Hamiltonian, the second-order susceptibility, and the SHG intensity result when the subscript h, for hole, is replaced by e, for electron, in Eqs. (10)–(16).

ACKNOWLEDGMENTS

We thank E. Burstein, E. Borguet, P. D. Kaplan, I. Koltover, and W. Theis for helpful discussions and A. Denenstein for technical help. We are particularly grateful to E. J. Mele for many stimulating discussions about the theory. This work was supported by the Office of Naval Research through Young Investigator program grant N00014-91-J-1867. A. G. Yodh also acknowledges partial support from the National Science Foundation, through Presidential Young Investigator program grant DMR-9058498 and Material Research Laboratory program grant DMR-8519059, and from the Alfred P. Sloan Foundation.

*Present address, Department of Chemistry, City College of New York, New York, New York 10031.

REFERENCES AND NOTES

1. E. Y. Wang, W. A. Albers, and C. E. Bliel, in *II–VI Semiconducting Compounds*, D. G. Thomas, ed. (Benjamin, New York, 1967), p. 136.
2. H. Shen, P. Parayanthal, F. H. Pollak, M. Tomkiewicz, T. J. Drummond, and J. N. Schulman, Appl. Phys. Lett. **48,** 653 (1986).
3. M. S. Yeganeh, J. Qi, A. G. Yodh, and M. C. Tamargo, in *Quantum Electronics and Laser Science*, Vol. 13 of 1992 OSA Technical Digest Series (Optical Society of America, Washington, D.C., 1992), p. 296; T. Zhang, Z. Xu, W. Lin, G. K. Wong, J. B. Ketterson, X. Wang, R. P. H. Chang, S. Liu, and M. M. Kappes, in *Quantum Electronics and Laser Science*, Vol. 13 of 1992 OSA Technical Digest Series (Washington, D.C., 1992), p. 262.
4. M. S. Yeganeh, J. Qi, A. G. Yodh, and M. C. Tamargo, Phys. Rev. Lett. **69,** 3579 (1992).
5. See, for example, H. H. K. Tom, T. F. Heinz, and Y. R. Shen, Phys. Rev. Lett. **51,** 1983 (1983); T. F. Heinz, M. M. T. Loy, and W. A. Thompson, Phys. Rev. Lett. **54,** 63 (1985); H. W. K. Tom and G. D. Aumiller, Phys. Rev. B **33,** 8818 (1986), and references therein.
6. J. F. McGilp and Y. Yeh, Solid State Commun. **59,** 91 (1986).
7. T. F. Heinz, F. J. Himpsel, E. Palange, and E. Burstein, Phys. Rev. Lett. **63,** 644 (1989).
8. M. S. Yeganeh, J. Qi, A. G. Yodh, and M. C. Tamargo, Phys. Rev. Lett. **68,** 3761 (1992).
9. L. Kassel, H. Abad, J. W. Garland, P. M. Raccah, J. E. Potts, M. A. Haase, and H. Cheng, Appl. Phys. Lett. **56,** 42 (1990).
10. K. Yokoyama and K. Hess, Phys. Rev. B **33,** 5595 (1986).
11. We have calculated that the density of carriers generated by two-photon absorption of the fundamental dye laser light is at least 4 orders of magnitude smaller than the density of the carriers generated by the photomodulating lamp light.
12. Our theoretical modeling was based on the integration of the one-dimensional Schrödinger equation for quantum-well potential. It showed that there existed six resonance states.
13. B. V. Zhuk, I. A. Zhukov, and A. A. Zlenko, Solid-State Electron. **29,** 247 (1986).
14. The other elements of the second-order susceptibility tensor

and the higher-order bulk contribution were measured to be negligible. For more detail, see M. S. Yaganeh, "Nonlinear optical spectroscopy of solid–solid interfaces," Ph.D. dissertation (University of Pennsylvania, Philadelphia, Pa., 1992).
15. S. Wang, *Solid State Electronics* (McGraw-Hill, New York, 1963).
16. N. V. Joshi, Phys. Rev. B **27,** 6272 (1983).
17. R. Shankar, *Principles of Quantum Mechanics* (Plenum, New York, 1985), p. 186.
18. See, for example, M. C. Tamargo, J. L. de Miguel, D. M. Hwang, and H. H. Farrell, J. Vac. Sci. Technol. B **6,** 784 (1988), and references therein.
19. M. S. Yeganeh, J. Qi, J. P. Culver, A. G. Yodh, and M. C. Tamargo, Phys. Rev. B **46,** 1603 (1992).